View metadata, citation and similar papers at core.ac.uk

brought to you by CORE

provided by Elsevier - Publisher Connector

Available online at www.sciencedirect.com

ScienceDirect

Energy Procedia 92 (2016) 180 – 187

Energy Procedia

6th International Conference on Silicon Photovoltaics, SiliconPV 2016

# Temperature dependent lifetime spectroscopy (TDLS) for the identification of metallic impurities

Etienne Quiniou, Olivier Palais*, Damien Barakel, Isabelle Périchaud

*Aix Marseille Univ, IM2NP, CNRS UMR 7334, Marseille, France*

**Abstract**

The paper is devoted to the identification of the metallic impurities in silicon wafers by using Temperature Dependent Lifetime Spectroscopy (TDLS). We consider the variation of all recombination mechanisms, intrinsic and extrinsic, to follow the variation of lifetime with the temperature. The extrinsic recombination mechanism is based on the standard Shockley-Read-Hall theory (SRH) [1], [2] and we simulated the variation of SRH lifetime for two impurities : gold and iron. The simulation results show that their SRH lifetime variations with the temperature are opposite and that the presence of a peak is characteristic of the impurity studied. Experimental measurements are displayed showing the identification of gold impurity by means of Phase-Shift TDLS (PS-TDLS) measurement. Thanks to these results, we demonstrate that PS-TDLS is an efficient method to identify gold and iron impurities at concentrations as low as $1.10^{10}cm^{-3}$ for a doping level of $1.10^{15}cm^{-3}$.

© 2016 The Authors. Published by Elsevier Ltd. This is an open access article under the CC BY-NC-ND license (http://creativecommons.org/licenses/by-nc-nd/4.0/).
Peer review by the scientific conference committee of SiliconPV 2016 under responsibility of PSE AG.

*Keywords:* Silicon ; Minority carrier lifetime ; Temperature ; Iron ; Gold

## 1. Introduction

After the elaboration and the purification process needed to make devices, semiconductor materials present numerous metallic impurities [3]. According to their natures and their concentrations, these impurities can degrade the material properties and in solar cells. Indeed, the conversion efficiency is limited by the charge carrier lifetime

* Corresponding author. Tel.: +33491288346.
*E-mail address:* olivier.palais@im2np.fr

1876-6102 © 2016 The Authors. Published by Elsevier Ltd. This is an open access article under the CC BY-NC-ND license (http://creativecommons.org/licenses/by-nc-nd/4.0/).
Peer review by the scientific conference committee of SiliconPV 2016 under responsibility of PSE AG.
doi:10.1016/j.egypro.2016.07.017

and/or by the increase of the phenomenon of Light Induced Degradation (LID). For example, in p-type silicon solar cells, an iron concentration of less than 1 ppm can reduce up to 40% the conversion efficiency [4].

Nowadays, bulk lifetime value of the minority carriers is a key parameter to evaluate the presence of recombinant defects. Deep Level Transient Spectroscopy (DLTS) turns out to be the most appropriate tool to characterize and identify these defects. Nevertheless this technique needs the preparation of a collecting structure which can modify the material properties and its detection capacity is limited to $10^{-4}$ multiplied by the doping level.

In this paper, we present a contactless method able to identify impurities at lower concentrations than DLTS (as low as $1.10^{10}$ at.cm$^{-3}$) and based on the carrier lifetime variations with temperature.

**Nomenclature**

| | |
|---|---|
| TDLS | Temperature Dependent Lifetime Spectroscopy |
| μW-PS | Microwaves Phase-Shift |
| PS-TDLS | Phase-Shift Temperature Dependent Lifetime Spectroscopy |
| SRH | Shockley, Read and Hall |
| LID | Light Induced Degradation |
| DLTS | Deep Level Transient Spectroscopy |
| $\tau$ | Lifetime (s) |
| C | Radiative coefficient band to band recombination (cm$^3$.s$^{-1}$) |
| n, p | Electron and hole concentration in non-equilibrium (cm$^{-3}$) |
| $n_0$, $p_0$ | Electron and hole concentration in thermal equilibrium (cm$^{-3}$) |
| $n_1$, $p_1$ | Electron and hole SRH density (cm$^{-3}$) |
| $\Delta n$, $\Delta p$ | Excess electron and hole density (cm$^{-3}$) |
| $C_p$ | Auger coefficient (cm$^6$.s$^{-1}$) |
| $g_{ehh}$ | Enhancement factor of the ehh-Auger process |
| $N_a$ | Concentration of dopant acceptors atoms (cm$^{-3}$) |
| $N_t$ | Impurity concentration (cm$^{-3}$) |
| $\sigma_{n,p}$ | Effective capture cross section of electrons and holes (cm$^2$) |
| $v_{th}$ | Thermal velocity (cm.s$^{-1}$) |
| $N_c$, $N_v$ | Effective densities of state at the conduction band and the valence band (cm$^{-3}$) |
| $E_t$ | Defect energy level (eV) |
| $E_c$, $E_v$ | Conduction and valence band edge energy (eV) |
| k | Boltzmann's constant (eV.K$^{-1}$) |
| T | Temperature (K) |
| CZ | Czochralski (silicon) |
| PECVD | Plasma-Enhanced Chemical Vapor Deposition |

## 2. Theory of temperature recombination's mechanism

The bulk lifetime measurement, whatever the setup, is an effective bulk lifetime $\tau_{b,eff}$ which takes into account the impact of intrinsic through radiative and Auger recombination and extrinsic recombination through mechanism described by SRH, as it is shown in the following equation:

$$\frac{1}{\tau_{b,eff}} = \frac{1}{\tau_{rad}} + \frac{1}{\tau_{Auger}} + \frac{1}{\tau_{SRH}} \quad (1)$$

Hence, the lifetime measurement with temperature requires the consideration of all the mechanisms of recombination and their variations with temperature.

### *2.1. Dependence of Radiative lifetime with temperature*

In the radiative recombination process, an electron recombines with a hole and transfers its excess energy and momentum to a photon. The radiative lifetime can write as:

$$\tau_{rad} = \frac{1}{C\left[\left(n_0 + p_0\right) + \Delta n\right]} \tag{2}$$

The C coefficient reflects the quantum-mechanical probability of a radiative transition. It depends strongly on the band structure of the semiconductor. Nelson and al. report $C_{Si}=10^{-15}$-$10^{-14}$ $cm^3s^{-1}$ for silicon while Landberg and al. [5] report $C_{GaAs}=10^{-10}$ $cm^3s^{-1}$ for GaAs. There are four orders of magnitude between direct and indirect gap materials. Equation (2) shows that the radiative lifetime depends on the inverse of the carrier density. So we can expect a sharp decline of $\tau_{rad}$ when the temperature increases.

### *2.2. Dependence of Auger lifetime with temperature*

Auger recombination is the second type of intrinsic recombination. In this process an electron recombines with a hole transferring its excess energy and momentum to another carrier. For p-type material, we describe the variation of Auger lifetime with temperature by means of the expression (3):

$$\tau^{p}_{Auger} = \frac{1}{g_{ehh} C_p N_A^2} \tag{3}$$

Altermatt and al. [6] and Hangleiter and al. [7] suggest an empirical temperature dependent relation for $C_p$ and $g_{ehh}$ respectively. For $C_p$ coefficient, the thermal dependence results from the addition of phonons which allows the momentum match of the carriers involved while the enhancement factor, $g_{eeh,}$ dependence take into account the properties of the exciton.

### *2.3. Dependence of the SRH lifetime with temperature*

The impact of extrinsic recombination via defects in the bulk was formulated by Shockley, Read and Hall in 1952. In this process, the presence of defects introduces discrete energy levels within the band gap. Such defect level can capture an electron and a hole from the respectively bands and the probability to capture a charge carrier depends on the nature of defects. The authors determined statistical recombination rate related to a single defect as a function of the excitation, material and defect parameters. Thus the recombination rate can write as:

$$U_{Auger} = \frac{np - n_i^2}{\left(p + p_1\right)\left[N_t \sigma_n v_{th}\right]^{-1} + \left(n + n_1\right)\left[N_t \sigma_p v_{th}\right]^{-1}} \tag{4}$$

The quantities $n_1$ and $p_1$ are the electron and hole concentrations when we consider that the trap level Et is situated at the level of fermi:

$$n_1 = N_c e^{\left(\frac{E_t - E_c}{kT}\right)} \quad \text{and} \quad p_1 = N_v e^{\left(\frac{E_v - E_t}{kT}\right)} \tag{5}$$

Assuming the charge neutrality $\Delta n = \Delta p$ and inserting the non-equilibrium concentrations $n = n_0+\Delta n$ and $p = p_0+\Delta p$, we can extract the SRH lifetime as:

$$\tau_{SRH} = \frac{\tau_{n0}\left(p_0 + p_1 + \Delta n\right) + \tau_{p0}\left(n_0 + n_1 + \Delta n\right)}{\left(p_0 + n_0 + \Delta n\right)} \tag{6}$$

The parameters $\tau_{n0}$ and $\tau_{p0}$ are the capture time constants of electrons and holes and can be expressed as

$$\tau_{n0} = \frac{1}{\sigma_n N_t v_{th}} \quad \text{and} \quad \tau_{p0} = \frac{1}{\sigma_p N_t v_{th}} \tag{7}$$

Where $v_{th}$ represents the thermal velocity of carriers and Nt, the defects concentration in $cm^{-3}$.
$\sigma_{n,p}$ are the capture cross-sections for electron and hole respectively. These parameters are characteristic, with their trap level, of an impurity and express the capability of an impurity to recombine carriers. The probability to capture a charge carrier can increase or decrease with the temperature following the nature of defects. We can classify the impurities according to the thermal dependence of their effective capture cross-section for which we obtain two models:

- $\sigma\left(T\right) = \sigma_\infty e^{\frac{-E_\infty}{kT}}$ (8)
- $\sigma(T) = \sigma_0 T^{-\alpha}$ (9)

Table I presents the recombination properties of some well described investigated impurities [8] which are representative of the contaminations present in the materials [4].

Table I. Published data for some impurities in p-type Si : trap level, capture cross-section of electron and hole at 300K, temperature dependence of σ are listed.

| Atom impurity | Trap level (eV) | $\sigma_n$ (300K) ($cm^2$) | $\sigma_p$ (300K) ($cm^2$) | σ(T) selected model [Ref.] |
|---|---|---|---|---|
| Cu | Ec-0,58 | $1.10^{-15}$ | $1.10^{-16}$ | (9) with α = 2 [9] |
| Ti | Ev+0,28 | $2,3.10^{-15}$ | $1,9.10^{-16}$ | (9) with α = 1,6 [10] |
| Ni | Ec-0,4 | $5,6.10^{-17}$ | $8.10^{-17}$ | (9) with α = 2,4 [11] |
| Au | Ev+0,34 | $5,18.10^{-16}$ | $1,5.10^{-15}$ | (9) with α = 2 [7] |
| Fe | Ev+0,38 | $3,6.10^{-15}$ | $7.10^{-17}$ | (8) with $E_\infty$= 0,024 [11] |

## 3. Results

### *3.1. Simulation results*

To ensure the possibility to identify an impurity by PS-TDLS method, we performed simulations on the lifetime evolution with temperature. Our simulations take into account all the recombination variations with temperature in the semiconductor material as a function of the doping level, the nature and concentration of impurity and the semiconductor type. Our model does not incorporate the variation of the surface recombination velocity which the variations with temperature are unclear; hence all the measurements were performed with surface passivation by means of oxide layers.

In the first step, we chose an impurity which properties are well known in silicon: gold in substitutional position. In p-type silicon, this impurity gives a deep level at 0.34eV above the valence band. Their carrier capture cross sections, indicated in Table 1, were measured at 77 and 300K by DLTS and PCD.

In the second step, we realized simulations of lifetime variations for iron impurity which has heavily recombinant behavior in interstitial position which is the main contaminant in silicon solar cell materials [3]. Its trap level is situated at 0.38eV above the valence band. Their carrier capture cross sections were measured by DLTS and TIDLS [10].

The variation of the intrinsic recombination lifetime with temperature and for four gold concentrations is shown in Fig. 1. These curves arise from our simulations for p-type Si doped at $1.10^{15}$cm-3 and for low-level injection. We observe that the intrinsic lifetime decreases when the temperature increases while the SRH lifetime of gold increases. At high temperature with gold contamination, a characteristic peak appears. This peak is the signature of gold impurity in lifetime spectroscopy with temperature. Nevertheless, at this temperature regime, the intrinsic lifetime decreases heavily and could mask the characteristic peak of gold.

Our simulations suggest that it is possible to identify the gold concentration up to a limit of $1.10^{10}$cm$^{-3}$. At a lower concentration, the intrinsic lifetimes are predominant with respect to the SRH lifetime.

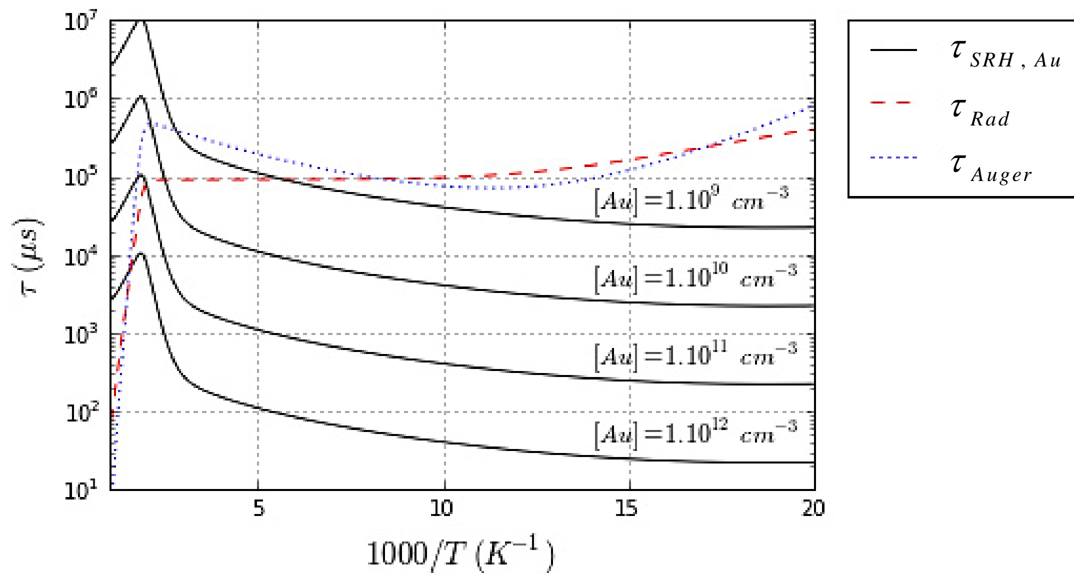


Fig. 1. Intrinsic and extrinsic lifetime versus temperature for four gold concentrations. Simulation realized for p-type Si doped at $10^{15}$cm$^{-3}$ in low-level condition $\Delta n=10^{14}$cm$^{-3}$.

Simulations presented in Fig. 2, were performed under the same conditions and show the impact of four iron different concentrations on the lifetime. The presence of iron in the material introduces a variation of the SRH lifetime completely different from that of gold. Indeed the lifetime decreases with temperature up to a peak at high temperature. The shape and the size of the peak are different from that of the previous figure and appear to be characteristic of iron impurity.

Note that compared to the intrinsic recombination, the identification is possible until $1.10^{11}$ atoms impurities per cm3.

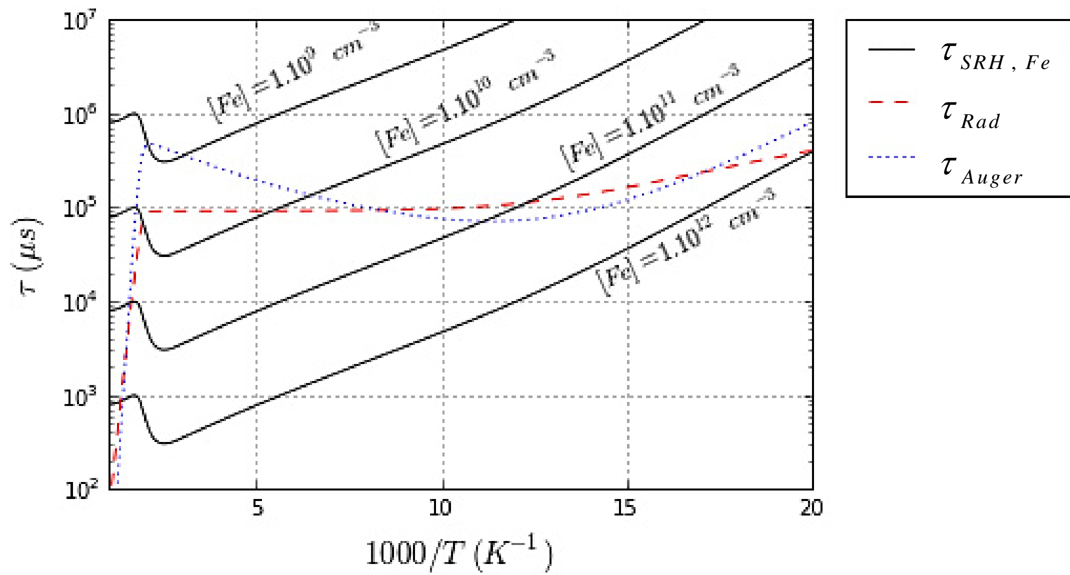


Fig. 2. Intrinsic and extrinsic lifetime versus temperature for four iron concentrations.

### 3.2. Experimental Setup

The materials investigated are:

- p-type CZ silicon wafer (10-20 ohm.cm). An oxide layer of a thickness of 120 nm was deposited by PECVD which is the optimal layer to reduce surface recombination velocities [12].
- p-type silicon wafer contaminated with gold

The lifetime was measured by the phase-shift measurement of reflected microwave (µW-PS) [13]. The sample is lighted with an intensity weak sine modulated light source leading to quasi continuous injection condition. The modulations of the pump create a change in the conductivity and so a change in the resistivity which is probed by microwaves. A detection system using a detector and a lock-in amplifier enables the measurement of the effective lifetime. The laser beam (lambda= 940 nm) intensity was chosen to satisfy low level excitation condition and the modulated frequency scan was performed from 1 kHz to 100 kHz.

The microwave frequency was 10 GHz. The phase-shift between the modulated frequency and the reflected microwave was analysed trough a lock-in amplifier.

To enable temperature dependent lifetime measurement, a liquid-nitrogen-cooled cryostat was integrated. The temperature was measured by two PT100 sensors with an accuracy of ±0.5°C. The first sensor was integrated in the heat exchanger controlling the temperature range of the cryostat from 100 to 425K. The control loop was realized by Lakeshore Temperature controller. The second PT100 is placed as closely as possible to the sample to take into account the decrease heat conductivity of the heat exchanger.

### 3.3. Experimental results

Fig. 3 presents the measured microwave phase-shift for two samples over a temperature range of 103.15 to 423.15 K which occurred at modulated frequency of 10 kHz.

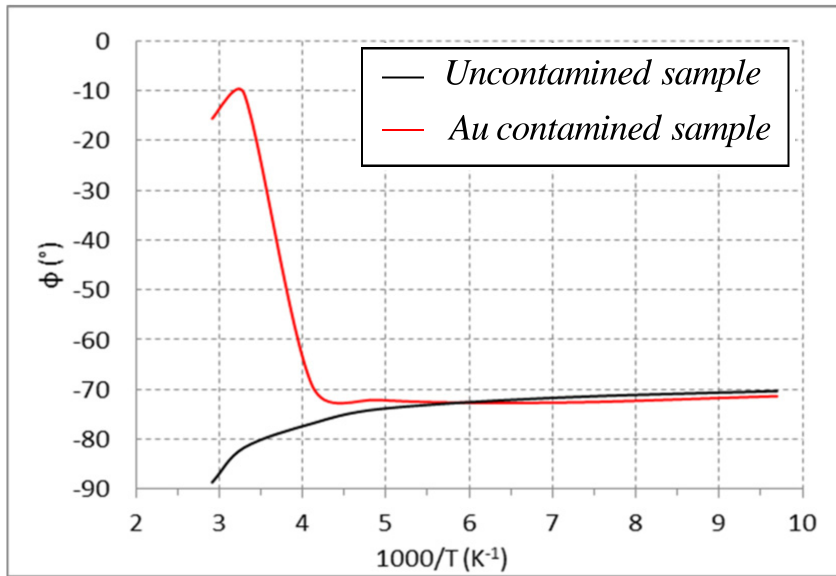


Fig. 3. Microwave phase shift as a function of temperature, measured on uncontaminated sample (black line) and gold contaminated sample (red line) at F=10kHz

For the uncontaminated sample, the phase-shift decreases slightly between -73 to -70° on a range of 5.5 to 10 $K^{-1}$. Then the decrease is more important, until -88°, on temperature range from 3 to 5.5 $K^{-1}$. No peak appears on our study temperature range. In the case of gold contaminated sample, the phase-shift is constant from 5.5 to 10 $K^{-1}$ and then sharply increases to a peak at -10° around 3.4$K^{-1}$. In absolute terms it corresponds to a decrease of the phase delay i.e. a decrease of the bulk lifetime. This decrease of the phase-shift involves an increase of the recombination phenomena of the previously created free carriers. Thus the lifetime of the contaminated sample is lower than uncontaminated sample. We attribute this lifetime decrease with the presence of gold impurity which is the main contaminant.

For the two samples, the phase-shift is constant from 5.5 to 10 $K^{-1}$. Thus the phase-shift measurement doesn't allow to detect the presence of gold impurity at temperatures below 5.5 $K^{-1}$ i.e. 182 K. Note that this result concerns only the gold impurity. Experiences are in progress to identify iron and copper impurities. The range of temperature allowing their identification depends on the nature of the impurity.

## 4. Conclusion

A contactless method for the identification of metallic impurities in silicon was presented by the means of the PS-TDLS. The theory of temperature dependent recombination's mechanisms in the semiconductors was examined. Using this previous theory and the literature's data for the recombinant properties of impurities, we performed simulations on the lifetime evolution with temperature. Indeed we have shown the capability of PS-TDLS to identify the impurity by its signature in spectroscopy lifetime over a temperature range of 50 to 500K. An identification of gold impurity was presented by a measure of the PS-TDLS.

## Acknowledgements

The authors would like to thank the French Agency for Environment and Energy Management (ADEME) which has supported this work.

## References

[1] W. Shockley, W. T. Read Jr. Statistics of the recombinations of holes and electrons. *Phys. Rev.* ;1952, 87. p. 835
[2] R. N. Hall. Electron-hole recombination in germanium. *Phys. Rev*.; 1952, 87, p. 387
[3] T. Buonassisi, A. A. Istratov, M. D. Pickett, M. Heuer, J. P. Kalejs, G. Hahn, M. A. Marcus, B. Lai, Z. Cai, S. M. Heald, T. F. Ciszek, R. F. Clark, D. W. Cunningham, A. M. Gabor, R. Jonczyk, S. Narayanan, E. Sauar, et E. R. Weber. Chemical natures and distributions of metal impurities in multicrystalline silicon materials. Prog. Photovolt. *Res. Appl*; 2006, p. 513‑531
[4] A. R. Peaker, V. P. Markevich, B. Hamilton, G. Parada, A. Dudas, A. Pap, E. Don, B. Lim, J. Schmidt, L. Yu, Y. Yoon, et G. Rozgonyi. Recombination via point defects and their complexes in solar silicon. *Phys. Status Solidi* A ; 2012. p. 1884‑1893
[5] P. T. Landsberg. Recombination in semiconductors. ; New York: *Cambridge University Press*, 1991
[6] P. P. Altermatt, J. Schmidt, G. Heiser, et A. G. Aberle. Assessment and parameterisation of Coulomb-enhanced Auger recombination coefficients in lowly injected crystalline silicon. *J. Appl. Phys*. ; 1997, p. 4938
[7] A. Hangleiter. Nonradiative recombination via deep impurity levels in silicon: Experiment. *Phys. Rev. B* ; 1987, p. 9149
[8] K. Graff. Metal Impurities in Silicon-Device Fabrication. Berlin, Heidelberg: *Springer*, 2000
[9] K. A. Moen. Modeling of minority carrier recombination and resistivity in sige bicmos technology for extreme environment applications. 2008.
[10] B. B. Paudyal, K. R. McIntosh, D. H. Macdonald. Temperature dependent carrier lifetime studies on Ti-doped multicrystalline silicon. *J. Appl. Phys*.; 2009, p. 124510.
[11] S. Rein. Lifetime spectroscopy a method of defect characterization in silicon for photovoltaic applications. Berlin; New York: *Springer*, 2005.
[12] M. J. Kerr. Surface, emitter and bulk recombination in silicon and development of silicon nitride passivated solar cells. 2002.
[13] O. Palais, A. Arcari. Contactless measurement of bulk lifetime and surface recombination velocity in silicon wafers. *J. Appl. Phys*.; 2003, p. 4686